Influence of source–sensor geometry on multi-source emission rate estimates

B.P. Crenna*, T.K. Flesch, J.D. Wilson

Department of Earth and Atmospheric Sciences, 1-26 Earth Sciences Building, University of Alberta, Edmonton, Alberta, Canada T6G 2E3

ABSTRACT

Multi-source emission rates inferred from measured concentrations using numerical dispersion models are often extremely sensitive to measurement and model error, rendering them unusable. This sensitivity to error is quantified by the condition number of the matrix of model-derived coefficients relating source strengths to concentrations. Using a dispersion model, we examine the dependence of this condition number on source–sensor geometry, atmospheric conditions, and the amount of concentration data included in the solution. Optimal sensor arrangements are those that measure source emissions (and background concentration, if it is unknown) as independently from each other as possible under the expected range of wind directions and atmospheric stabilities. Although including more concentration measurements can improve the emission inferences, the benefit is highly contingent upon sensor placement. A set of recommendations to minimize sensitivity to error is presented. This includes arranging sensors so that each detects emissions from as few sources as possible; keeping sensors separated, both horizontally and vertically, to benefit from asymmetries in source distribution and surface layer structure; using more measurements in a given calculation, either by adding more sensors or by incorporating data from different times; and using dispersion models to assess condition number and guide sensor placement before and during a field study.

© 2008 Elsevier Ltd. All rights reserved.

1. Introduction

Because it can be difficult to directly measure trace gas fluxes from distributed sources, emission rates are commonly estimated indirectly from predictions made by numerical dispersion models (e.g. Wilson et al., 1982; Raupach, 1989a; Flesch et al., 1995). When provided with concentration measurements obtained in the vicinity of a single source, models can infer with reasonable accuracy the source strength required to produce the given concentrations (for experimental verification, see e.g. Flesch et al., 2004). When more than one source is present, or where a single emitting surface is highly inhomogeneous, the objective may be to determine multiple emission rates. Here, we shall refer to these as *multi-source problems*.

Many real-world emission sites are a composite of sources. For example, a farm may be a significant source of gases to the atmosphere, with emissions from barns, animal waste lagoons, outdoor animal pens, food stocks, etc. It can be practically difficult (and scientifically challenging) to make isolated measurements of emissions from these components. Other sources, such as field crops, are of a single type but are spatially variable to the extent that a quantification of this variability is valuable.

Unfortunately, emission rate estimates for multi-source problems are often badly behaved, with spurious predictions obtained comparably often to appropriate values (e.g. Raupach, 1989b). Consider a multi-source problem in which *n* concentration sensors are located in proximity to

* Corresponding author.
E-mail address: brian@thunderbeachscientific.com (B.P. Crenna).

m sources, each source having its own emission rate Q_j ($j = 1, …, m$). Each source can potentially contribute to the signal (C_i, $i = 1, …, n$) seen by each sensor, the amount depending on the state of the atmosphere between source and detector. This relationship can be determined by an atmospheric dispersion model and expressed as a coefficient a_{ij}, so that concentration C_i is the superposition of products $a_{ij}Q_j$, plus any background concentration C_{BG}. The result is a linear system of equations:

$$a_{ij}Q_j + C_{BG} = C_i \tag{1}$$

which can be solved using standard numerical techniques to calculate Q_j. The emission sources can be arbitrarily complex in shape (elevated and/or on the surface), provided the dispersion model is capable of correctly associating their emissions to concentration.

A solution to system (1) exists if and only if there are at least as many equations as unknowns; we must therefore provide at least as many suitable concentration measurements as unknowns (here being the m emission rates and possibly C_{BG}). Of course, we can include more equations than unknowns; though the solution then becomes a best-fit in a statistical sense, rather than being unique.

Under certain conditions, this system can amplify minor errors in measured concentrations C_i and/or model-derived coefficients a_{ij} by many orders of magnitude. A system is said to be *ill-conditioned* if small changes in its data result in large changes in its solution, and *well-conditioned* otherwise. This sensitivity is quantified by the *condition number* κ of the $m \times n$ matrix of coefficients a_{ij}. Many introductory texts in applied linear algebra (e.g. Scheick, 1996) provide numerical examples of ill-conditioning in simple systems.

The problem of ill-conditioning in equations relating source emission rates to concentrations has been explicitly examined in previous studies. It arose in analyses of the source–sink distribution of scalar quantities within plant canopies (e.g. Raupach, 1989a; Hsieh et al., 2003; Wohlfahrt, 2004; Simon et al., 2005; Qiu and Warland, 2006), in which a (nominally) horizontally uniform plant canopy was divided into m discrete layers whose unknown emission rates were related to a vertical profile of n concentration measurements using numerical dispersion models. This problem is characteristically ill-conditioned, and various approaches have been used to handle the difficulties that this causes. Raupach (1989b) recommended that n exceed m to reduce the effect. Leuning et al. (2000) applied a standard method of solution called *singular value decomposition* (SVD) (Press et al., 1986) as a fitting procedure to reduce error sensitivity; while Siqueira et al. (2000) added a smoothness constraint on the predicted source profiles to further improve the solutions.

Roussel et al. (2000) provided a thorough analysis of the condition number problem for estimating deposition rate from multiple sources, and suggested a technique that requires extra concentration data to obtain a solution in poorly conditioned cases. Haupt (2005), Haupt et al. (2006), and Allen et al. (2007a,b) examined ill-conditioning in a system of equations similar to Eq. (1). They used a "genetic algorithm" to seek a solution to a highly over-determined system created by introducing concentrations

measured over an extended period of time. We might expect from statistical reasoning that as more information is added to the system, the solution should improve.

In earlier studies, little has been said about the influence of concentration sensor placement on sensitivity to error in the solutions. This is potentially an important factor for real-world applications, since sensor positioning is under an experimentalist's control. In some locations, a given sensor might detect emissions from only one source; while in others, it will intercept emissions from several sources at the same time. We shall refer to the relative positioning between sensors and sources as *source–sensor geometry*. Modifying this geometry will affect the coefficients of the system of equations to be solved and, therefore, its condition number κ. Changes in environmental variables such as wind direction and atmospheric stability alter the effective sensor positions within the source plumes and will cause effects equivalent to physically moving them.

In this paper, we will examine how source–sensor geometry and meteorological conditions can affect κ, in a set of dispersion model-generated test cases involving area sources at the surface. In addition, we will briefly examine the effect of increasing the number of equations in the system by deploying more sensors. From these studies, we will infer a set of general guidelines for use when estimating multiple source strengths from measured concentrations.

2. Algebraic formulation

In a multi-source problem, we can express the governing system of equations (1) in vector notation as

$$\boldsymbol{AQ} + \boldsymbol{C_{BG}} = \boldsymbol{C} \tag{2}$$

where $\boldsymbol{A}$ is the $m \times n$ matrix of model coefficients, $\boldsymbol{C}$ is the vector of n observed concentrations, and $\boldsymbol{C_{BG}} = C_{BG}\boldsymbol{r}$, where $\boldsymbol{r}$ is a vector whose n components are all one. We assume that C_{BG} is spatially uniform but may vary from one measurement interval to the next. We can derive a relation for condition number κ by considering the effect of perturbations $\delta\boldsymbol{C}$ on the vector $\boldsymbol{C}$ of measured concentrations and $\delta\boldsymbol{A}$ on the $m \times n$ matrix $\boldsymbol{A}$ of model-derived coefficients, which we presume causes an error $\delta\boldsymbol{Q}$ in our calculated source strengths $\boldsymbol{Q}$. Introducing these perturbations to Eq. (2) and performing standard matrix operations, we find that the sensitivity of the overall system of equations to measurement and modeling error is bounded by

$$\frac{\|\delta\boldsymbol{Q}\|}{\|\boldsymbol{Q}\|} \leq \kappa \left(\frac{\|\delta\boldsymbol{A}\|}{\|\boldsymbol{A}\|} + \frac{\|\delta\boldsymbol{C}\|}{\|\boldsymbol{C}\|} + \frac{\|\delta\boldsymbol{C_{BG}}\|}{\|\boldsymbol{C_{BG}}\|} \right) \tag{3}$$

where condition number $\| \boldsymbol{A} \| \, \| \boldsymbol{A}^{-1} \|$ is the amplification factor relating perturbations to changes in emission rate $\delta\boldsymbol{Q}$ and (for this study). $\| \boldsymbol{A} \|$ is the so-called l_2 norm of coefficient matrix $\boldsymbol{A}$. This norm is selected because it appears in the standard SVD technique we use to solve the systems.

Eq. (3) implies that the relative errors in the estimated emission rates are amplified by the condition number κ. However, it is important to note that κ gives only an upper bound to the relative error $\| \delta\boldsymbol{Q} \| / \| \boldsymbol{Q} \|$, rather than being

sufficient as a measure to determine the sensitivity of the system to error (Noble and Daniel, 1988). In other words, although small κ does guarantee that the system is insensitive to error, a large value of κ does not guarantee sensitivity to error. We must therefore be somewhat cautious in our interpretation of large κ where it occurs.

A particularly misleading source of unreasonably large κ is referred to as *artificial ill-conditioning* (Gentle, 1998). Numerically, this can occur when the elements in one row or column of the matrix are significantly different in scale from the other elements. In calculating condition number, the ratio of large to small a_{ij} can lead to high κ even where it does not imply a marked sensitivity to perturbations. Artificial ill-conditioning reduces the usefulness of κ as a diagnostic of error sensitivity, and we must consider the potential for its occurrence in a given experiment. In the case studies to follow, we will test for this explicitly in some cases.

3. Modeling studies

We will examine a set of model-generated scenarios in which background concentration and/or one or more unknown ground-level area source strengths are determined from measured concentrations. In this study, the positions and shapes of all area sources are assumed to be known and unchanging. The size, location, and strengths of the sources are mostly arbitrary but have been chosen to illustrate general cases. The general principles we derive from these studies will be applicable to measure a wide range of sources (e.g. distributed within plant canopies, localized at points, etc.) and not restricted to area sources alone.

We use a numerical model implementing the Flesch et al. (2004) Lagrangian stochastic (LS) or particle-following scheme to relate measured concentrations to the emission rates from surface area sources. LS models are arguably the most natural or realistic of existing dispersion models for this type of problem (Wilson and Sawford, 1996). Like all LS schemes, our model introduces unavoidable error because its predictions are generated by ensembles of randomized particle trajectories. For most of the studies in this paper, very large numbers of particles (up to 10^9) are used and the model error is kept much smaller than any noise added intentionally to our concentration measurements. Model error also arises unavoidably because numerical models are based on idealized relationships that are only an approximation of the real world. Such idealizations presumably introduce systematic errors in a_{ij}, but it is outside the scope of this paper to attempt to address such errors.

Our goal is to vary the positions of a set of concentration sensors and/or the atmospheric state and observe resulting changes in the condition number, which we compute from the coefficients provided by our numerical model. In some cases, we will also assess the system's response to noise in a specific geometry. To do this, we first assume that the source strengths are known and use the model to predict concentrations at the locations of our sensors. These predicted concentrations are then used to back-calculate the source emission rates, with noise of specified amplitude being added to the concentrations.

3.1. Case 1: single unknown source with unknown background concentration

The simplest case in which condition number exerts an influence on estimates is that of a single source with unknown emission rate Q and unknown background concentration C_{BG}. This is perhaps the most common situation in field experiments and, as we shall see, it is prone to artificial ill-conditioning. Because there are two unknowns, at least two concentration measurements are required for a solution; for two sensors, system (1) in matrix form becomes

$$\begin{bmatrix} a_{\mathrm{f}} & 1 \\ a_{\mathrm{m}} & 1 \end{bmatrix} \begin{bmatrix} Q \\ C_{\mathrm{BG}} \end{bmatrix} = \begin{bmatrix} C_{\mathrm{f}} \\ C_{\mathrm{m}} \end{bmatrix} \tag{4}$$

in which C_{f} and C_{m} are the measured concentrations and coefficients a_{f} and a_{m} are model-derived parameters relating these concentrations to Q.

The column of 1's in the matrix is responsible for the potential occurrence of artificial ill-conditioning; it will arise if a_{f} and a_{m} are of similar size and are both either much smaller or much larger than unity. This can occur trivially by the choice of units for concentration, wind speed, and emission rate. Model coefficients will be smallest whenever the source has only a weak influence on concentration at either sensor's location. This will happen outside and at the edge of the source plume and if the source area is small relative to the sensor's concentration footprint. The latter can arise either because the source is intrinsically small or when the concentration footprint grows large in unstable atmospheric conditions that broaden horizontal dispersion.

Gentle (1998) states that there is no general procedure to determine if ill-conditioning is artificial or real. Fortunately, it is possible to reduce potential artificial ill-conditioning in this case by rescaling the left column to match the 1's, replacing the system by

$$\begin{bmatrix} \dfrac{a_{\mathrm{f}}}{b} & 1 \\ \dfrac{a_{\mathrm{m}}}{b} & 1 \end{bmatrix} \begin{bmatrix} bQ \\ C_{\mathrm{BG}} \end{bmatrix} = \begin{bmatrix} C_{\mathrm{f}} \\ C_{\mathrm{m}} \end{bmatrix} \tag{5}$$

where

$$b = \begin{cases} \min(a_{\mathrm{f}}, a_{\mathrm{m}}) & \text{if } a_{\mathrm{f}} \neq 0 \text{ and } a_{\mathrm{m}} \neq 0 \\ \max(a_{\mathrm{f}}, a_{\mathrm{m}}) & \text{if } a_{\mathrm{f}} = 0 \text{ or } a_{\mathrm{m}} = 0 \end{cases} \tag{6}$$

We consider a test case in which the source is a 100 m diameter circle with a surface roughness of 0.01 m, a Northerly wind (friction velocity u_* of $1\,\mathrm{m\,s^{-1}}$), and surface layer stratification ranging from very stable ($L = +10$ m) to very unstable ($L = -5$ m). The emission rate Q is assumed to be $100\,\mu\mathrm{g\,m^{-2}\,s^{-1}}$ and the background concentration[1] C_{BG} is $100\,\mu\mathrm{g\,m^{-3}}$. Two sensors are placed 1.5 m above the surface: one sensor remains stationary 100 m downwind from the trailing edge of the source, while the other is placed at various locations to generate

---

[1] In these examples, we have used units of gas density ($\mu\mathrm{g\,m^{-3}}$) rather than gas concentration (ppmv, ppbv).

a plot of κ as a function of its position. Note that the specifics are completely arbitrary and have no bearing on the general conclusions.

The sensors are optimally placed with one upwind of and outside the source plume and the other downwind and within the plume (Fig. 1a), because it fully separates the measurements needed to infer the two unknowns. The system in matrix form then reduces to:

$$\begin{bmatrix} a_f & 1 \\ 0 & 1 \end{bmatrix} \begin{bmatrix} Q \\ C_{BG} \end{bmatrix} = \begin{bmatrix} C_f \\ C_m \end{bmatrix} \tag{7}$$

in which C_f and C_m are measured by the downwind and upwind sensors, respectively. For this arrangement, we note that the potential for both real and artificial ill-conditioning occurs as $a_f \to 0$. If the upwind sensor is moved into the plume (Fig. 1b), κ increases because both sensors detect an increasingly similar combination of background- and source-derived tracer.

Fig. 2 plots κ as a function of the location of the moveable sensor under different stabilities. In all cases, the κ distributions (shaded) are symmetrical and have maxima at the position of the fixed sensor, meaning that predictions using data from co-located sensors are most sensitive to error. Irregularities in the shading are artifacts generated by contouring κ values calculated on a finite grid and by model uncertainty. The teardrop-shaped maxima follow the concentration contours (lines) at which both sensors see the same concentration C, implying that inferred source strengths are most sensitive to error whenever their measured concentrations are the same. This becomes obvious when we consider that under such conditions the system is

$$a_f Q + C_{BG} = C$$
$$a_m Q + C_{BG} = C \tag{8}$$

which implies that $a_f = a_m$ and therefore $\kappa \to \infty$. Although not shown, the resultant patterns are qualitatively similar when the test sensor's height differs from that of the stationary sensor.

In the unstable case shown in Fig. 2c, κ is slightly larger when the test sensor is upwind of the source than when it is a short distance downwind. This is weak artificial ill-conditioning caused by a reduction in a_f in Eq. (7); no real increased sensitivity to error exists. It arises because greater lateral dispersion in the unstable case widens the fixed sensor's concentration footprint, reducing the source's influence on C_f and decreasing a_f. When the moveable sensor is placed just downwind of the source, it measures higher concentrations than the fixed sensor and a_m exceeds a_f sufficiently to reduce κ.

Because κ is only an upper bound on error response and artificial ill-conditioning can occur, it is helpful to observe the actual response of emission rate estimates to changes in concentration. With the sensors placed as shown in Fig. 1a, if we reduce C_f by 10%, the predicted Q decreases by 14% and C_{BG} remains correct. We note that for this geometry, $|\delta Q|/Q \approx |\delta C_f|/C_f$. Moving the test sensor into a position where $\kappa \sim 1500$ (Fig. 1b), we find that a much smaller 1% reduction in C_f results in spurious predictions of $-40\ \mu g\ m^{-2}\ s^{-1}$ for Q and $2180\ \mu g\ m^{-3}$ for C_{BG}; now, $|\delta Q|/Q \gg |\delta C_f|/C_f$ and $|\delta C_{BG}|/C_{BG} \gg |\delta C_f|/C_f$.

We next vertically align two point concentration sensors on a tower placed at various distances downwind of the same source (Fig. 1c). One sensor remains fixed at 0.5 m above the surface while the other sensor's height is varied from 1 m to 10 m. Fig. 3 shows κ as a function of both the tower's distance from source center and the moveable sensor's height, for three surface layer stabilities. In each case, κ increases with the tower's distance downwind of the source and decreases as the separation between sensors grows. The lowest κ values occur for stable stratification, where the higher sensor is located above the source plume and reads C_{BG} directly. Conversely, unstable stratification leads to the largest κ, because the concentration is similar at all heights considered and little new information is
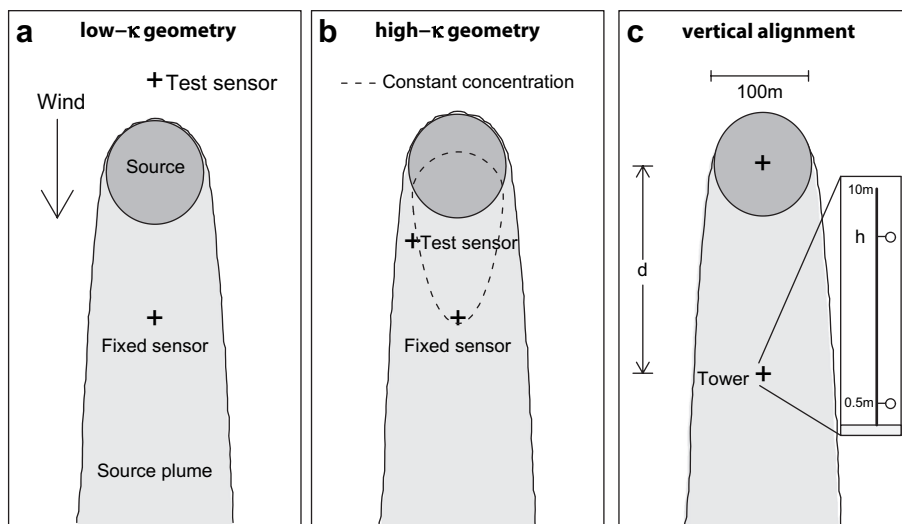
Fig. 1. Placement of two concentration sensors relative to a circular area source. In all cases, wind is from the North. (a) Test sensor is placed upwind of the source. (b) Test sensor is moved to a location with concentration similar to that near the fixed sensor. (c) Both sensors are placed on the same tower.
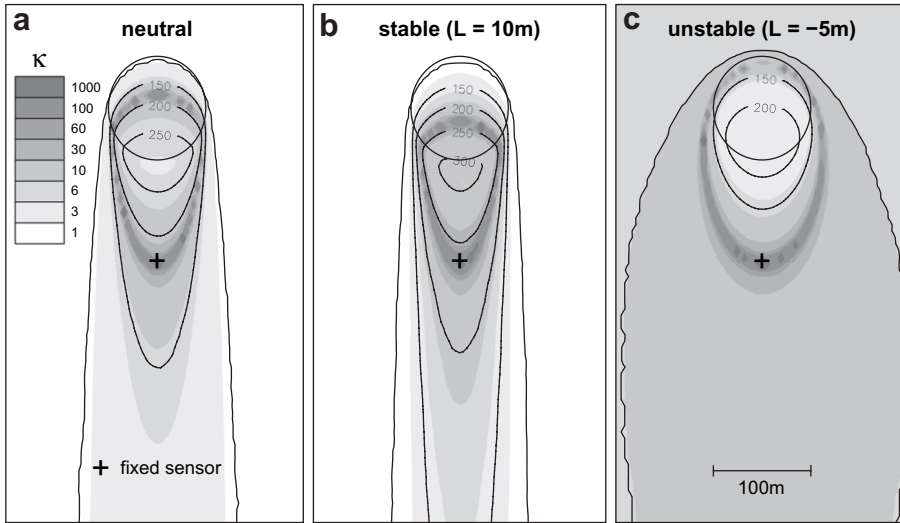
Fig. 2. Contours of concentration (in $\mu g\,m^{-3}$) at 1.5 m above the surface in the region of the circular area source, and the computed condition number κ (shading) as function of the position of the detector relative to the source.

provided by the second sensor. For all stratifications, large κ values downwind of the source imply that attempts to estimate both Q and C_{BG} using two vertically aligned sensors on a 10 m tower placed well downwind are likely to suffer from sensitivity to error.

It is evident from each of the above experiments that the optimal arrangement is generally to measure the background concentration as independently as possible from the localized source. It is also important to place sensors so that they are unlikely to measure similar source emissions.

3.2. Case 2: two unknown sources with known background concentration

Figs. 4 and 5 show hypothetical cases in which two circular area sources both emitting $100\,\mu g\,m^{-2}\,s^{-1}$ of an arbitrary tracer are located near each other. We consider two extremes of source–sensor geometry: in Fig. 4, the fixed sensor is positioned so that the sources are antisymmetric relative to its position and the wind direction; in Fig. 5, the sources are aligned symmetrically. Our goal is to determine their separate emission rates Q_1 and Q_2, assuming for simplicity that C_{BG} is known ($100\,\mu g\,m^{-3}$). Because there are two unknowns, at least two sensors are again required; for clarity, we use only the minimum number. As before, one point sensor is placed 100 m downwind from the sources and remains stationary, while the second sensor is moved to various locations to observe the effect of its position on κ. In this case, the system becomes

$$\begin{bmatrix} a_{f1} & a_{f2} \\ a_{m1} & a_{m2} \end{bmatrix} \begin{bmatrix} Q_1 \\ Q_2 \end{bmatrix} = \begin{bmatrix} C_f - C_{BG} \\ C_m - C_{BG} \end{bmatrix} \tag{9}$$
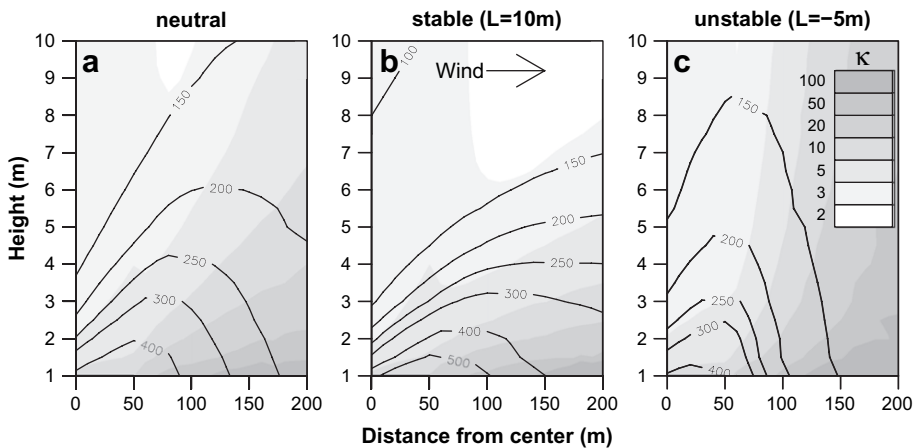
Fig. 3. Condition number (shading) and concentration contours (in $\mu g\,m^{-3}$) as a function of distance downwind of the source center and height of the moveable sensor above the surface in Fig. 1c; one sensor remains fixed at a height of 0.5 m. For all stratifications, κ increases with distance from the source and decreases as the height of the movable sensor increases.
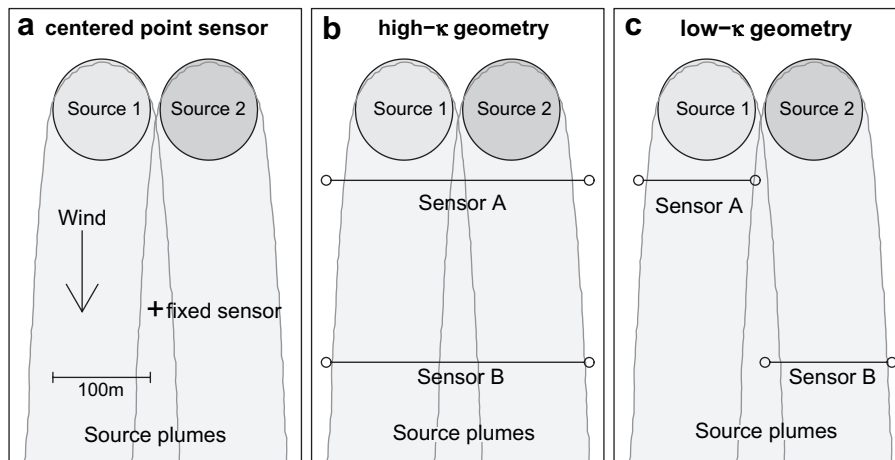
Fig. 4. Placement of sensors near two circular area sources that are antisymmetric relative to the sensor location and wind direction, with C_{BG} assumed to be known: (a) stationary point sensor located on center line between sources; (b) two line sensors intercept both source plumes, resulting in large κ; (c) two line sensors intercept single-source plumes, giving lower κ.

and does not suffer in general from artificial ill-conditioning.

Fig. 6 plots κ as a function of the second or "probe" sensor's position for the antisymmetric source arrangement. For each placement of the fixed sensor, κ grows without bound as the second sensor is moved outside both source plumes and the system becomes undetermined. When the stationary sensor is placed on the axis of symmetry between the sources (Fig. 6a), κ is large along the axis and decreases away from it, with secondary maxima near the locations of greatest concentration. Although not shown, the distribution remains qualitatively the same if the second sensor's height is increased to 3 m.

If the stationary sensor is placed directly downwind of one source (Fig. 6b), the κ distribution becomes asymmetrical, reaching a maximum at the position of the first sensor (i.e. when the sensors are co-located) and a minimum

when the second sensor is placed directly downwind of the other source. This confirms our expectation that κ should be smallest when each sensor detects emissions from only one source. A change in wind direction (Fig. 6c) effectively shifts the centrally located fixed sensor's position laterally relative to the sources and creates a similar pattern to Fig. 6b. Clearly, changes in wind direction can affect the system's potential sensitivity to error with no changes to source or sensor.

We next consider the same antisymmetric source arrangement but with point sensors replaced by line-averages, as shown in Fig. 4b and c. When both line sensors are placed to intersect the full width of the source plumes (Fig. 4b), κ is calculated to be 1900. For this geometry, when C_m is reduced by 1%, predicted emission rates Q_1 and Q_2 change dramatically from the correct 100 μg m^{-2} s^{-1}, with Q_1 estimated as -269 μg m^{-2} s^{-1} and Q_2 increasing to
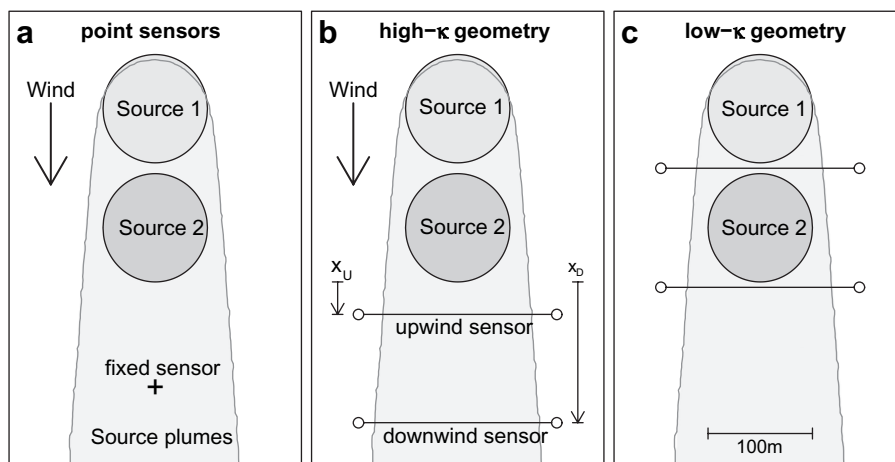
Fig. 5. As in Fig. 4, but for sources located symmetrically relative to sensor placement and wind direction. Condition number is large when both sensors are placed downwind of the two sources, and smallest when each sensor is situated near the downwind edge of a single source.
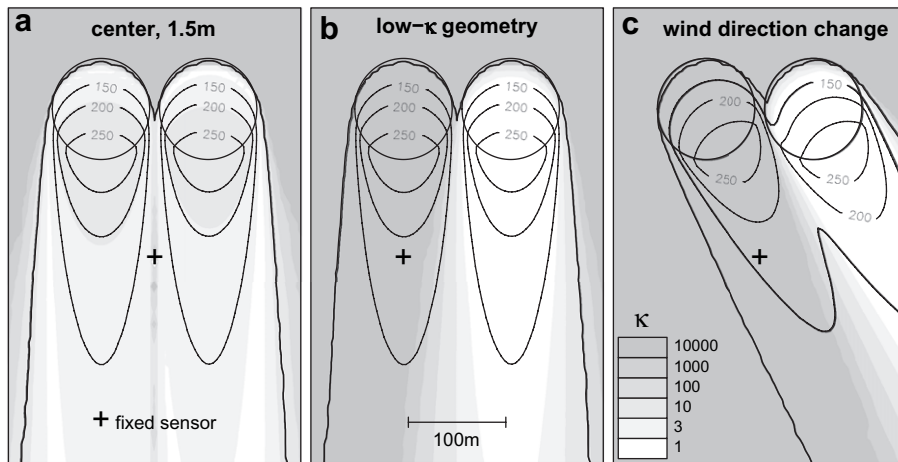
Fig. 6. Plots of condition number for the two area sources in Fig. 4 under neutral stability. A stationary sensor is placed at the location of the + symbol and the second is moved over the entire plot domain. Both sensors are at height 1.5 m.

$463 \, \mu\text{g m}^{-2}\,\text{s}^{-1}$. Varying the height of one or both line sensors yielded no significant reduction in the sensitivity, because the two source plumes are similar at all heights.

If the sensors are relocated so that each sees only one source (Fig. 4c), κ drops to just 1.66. Reducing C_A by 10% now decreases the upwind source's estimated strength Q_1 by a similar fraction, while Q_2 decreases by less than 1%. The system now behaves like two nearly independent single-source problems; an insignificant coupling arises because both sensors intercept the plume edges. Of course, this coupling will increase when the plumes widen in unstable conditions and when the wind direction transports one plume further into the domain of the other sensor.

Figs. 7 and 8 show the κ distribution for the symmetric source arrangement. We note first that κ is relatively large everywhere downwind of both sources, independent of stability and the probe sensor's height. This implies that it might be difficult to distinguish the two sources using only sensors placed well downwind of both. Condition number decreases as the probe sensor is moved to where it detects only the upwind source. Although κ is smallest near the center of the upwind source for neutral stratification (Fig. 7a), a region with $\kappa > 5$ occurs there for unstable stratification (Fig. 7b). We infer that a sensor arrangement appropriate for one stability class might be unsuitable for another. Fortunately, κ is small for all stratifications when the sensors are both located near the downwind edges (Fig. 8).

In Fig. 7c, we note that if one sensor is placed much higher than the other (5 m vs. 1.5 m), the region of low κ is much larger than when both sensors are at the same height, but its minimum value is larger. Although the source symmetry is now partially offset by the atmosphere's vertical inhomogeneity, placing the sensors at different heights does not greatly improve our ability to distinguish the emissions from a location well downwind of both.

Finally, we place line sensors at various locations relative to the symmetric sources as illustrated in Fig. 5b and c and compute κ for each placement. The results for neutral

stratification are shown in Fig. 9, with the position of the sensor initially further upwind plotted along the x axis and the position of the other sensor along the y axis. The patterns are found to be qualitatively similar for other stratifications. With both sensors at the same 1.5 m height (Fig. 9a), κ is at its minimum when one sensor is placed near the downwind edge of each source; it is impractically large for all arrangements in which the sensors are both downwind of all sources and infinite whenever they are collocated. Placing the sensors at different heights (1 m and 3 m) shifts the pattern somewhat (Fig. 9b), but as before, large κ occurs if both sensors are placed downwind of both sources. We conclude that attempting to separate two sources from a downwind location is unlikely to succeed in the symmetric case.

3.3. Including additional concentration measurements

We next briefly examine the consequences of increasing the number n of concentration measurements beyond the number m of unknown sources. We might expect that sensitivity to error in the emission rate estimates will be reduced as redundant measurements are included; the solution becomes a best-fit to the data rather than being constrained to exactly match all measurements.

Data can be added to the system either by deploying more sensors or by including observations taken at different times. As mentioned earlier, Raupach (1989b) found that increasing the number of concentration sensors reduced sensitivity to error in a plant canopy emission rate study. Of course, there are practical limits to this approach (e.g. sensor cost). Haupt (2005) augmented the system with concentration measurements made over a period of time, rather than concurrently. This approach requires that we assume that the source strength is either constant or varies predictably. Data from other times can be used even if the wind and stratification change, provided the model relating emission rates to concentrations remains valid. In effect, we expect the method to reduce measurement error by increasing the number of observations.
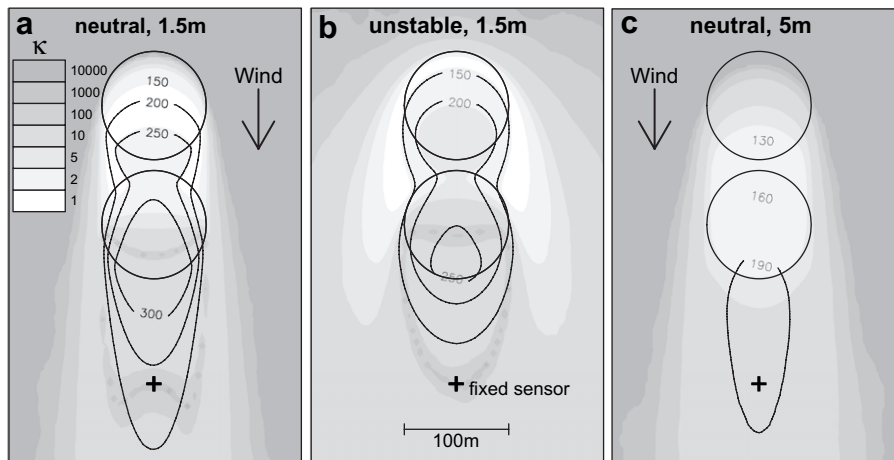
Fig. 7. Condition number for the area sources in Fig. 5a. In plots a and b, both sensors are at height 1.5 m; in c, the test sensor is at 5 m. Concentration contours (lines) are at the height of the test sensor. Note that κ is fairly large everywhere downwind of the sources and there is no position with low κ for all stratifications.

In the following numerical experiments, we observe changes in condition number κ as additional sensors are placed near unknown sources identical to those in two of the previous experiments. In the first, we add sensors to the vertical profile in Fig. 1c, with two sensors remaining fixed at 0.5 m and 10 m and up to nine additional sensors being spaced evenly between these two extremes. The profile is positioned 100 m directly downwind of the source. The results, seen in Fig. 10a, might be unexpected: κ remains nearly constant despite the extra sensors and actually slightly increases as more are added. Surprisingly, we would be better off using just two sensors placed well apart rather than introducing more sensors between the two.

In the second scenario, a horizontal array of line sensors is placed perpendicular to the wind from 0 m to 200 m downwind of the two symmetrically arranged sources in Case 2 (Fig. 5b). Again, two sensors remain fixed at the end locations and up to nine additional line sensors are spaced evenly in the gap between them. An experimenter,

determined to distinguish the two sources but for some reason unable to place the sensors optimally (as in Fig. 5c), might hope to reduce sensitivity to noise by increasing the number of downwind measurements. Given the results shown in Fig. 10b, we see that the attempt would not meet with much success. Although additional sensors provide some benefit in unstable conditions, with κ decreasing from 58 to 20 as the number of sensors grows from two to 11, it generally remains fairly large.

From these two examples, it is clear that adding more sensors without careful consideration of their geometry is not guaranteed to improve sensitivity to error.

4. Discussion

There are three basic means by which we can improve our emission rate predictions in light of the observed sensitivity to measurement and model errors:
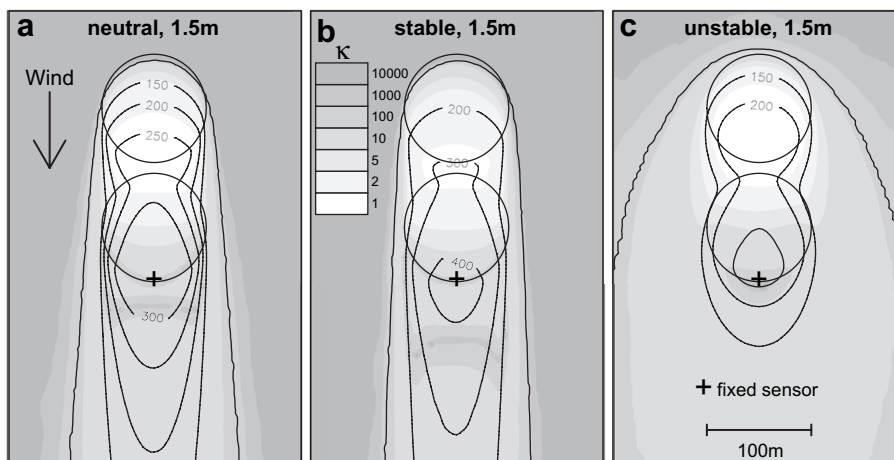
Fig. 8. Condition number for the sources in Fig. 5a, with the stationary sensor moved to the edge of the downwind source. Now, κ is low near the edge of the upwind source for all stratifications.
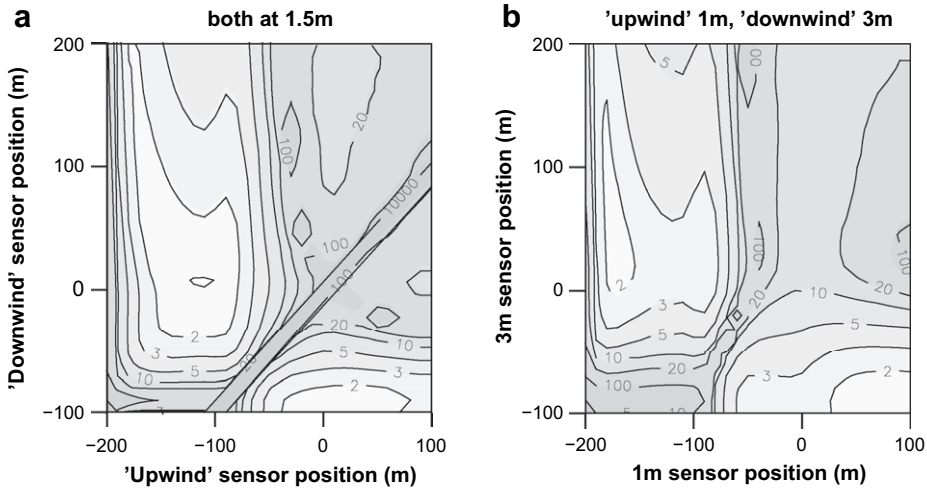
Fig. 9. Condition number for the area sources in Fig. 5b and c as a function of the downwind distance from source 2 of two line sensors. (a) With both sensors at height 1.5 m, minimum κ occurs when one sensor is positioned near the downwind edge of each source, as in Fig. 5c; $\kappa \rightarrow \infty$ whenever the two sensors are collocated (diagonal line at lower right.) (b) With one sensor placed 1 m above the surface and the other at 3 m, maximum κ no longer occurs when the sensors are collocated. In each case, κ is large whenever both sensors are downwind of both sources.

(1) Most obviously, we can ensure that measurement and modeling errors are kept as small as possible. Measurement averaging time must be sufficiently long to minimize noise in the data, while remaining within the order 15–60 min averaging times implicit in meteorological correlations underpinning the dispersion model's algorithms (e.g., Flesch et al., 2004). When using LS models, coefficient error caused by the inherent randomness in such models can be reduced by increasing the number of particles released, to the extent possible within available computation time. Of course, error due to mismatch between real-world flow and idealized model flow cannot be reduced, except (perhaps) by selecting more physically realistic parameterizations.

(2) We can seek to reduce the condition number of the coefficient matrix $\boldsymbol{A}$, typically by decreasing the likelihood that equations within the system will be linearly dependent. In the present context, this implies that to the extent possible, the concentration sensors must be placed so as to detect only one source at a time, while ensuring that all sources are observed; and that sensors remain physically separated from each other, so that the relationships between local concentrations and emission rates are dissimilar. As the real-world setup diverges from this arrangement, the emission rate estimates become more error-sensitive.

(3) We can invoke different solution techniques and constraints to overcome the effects of a large condition
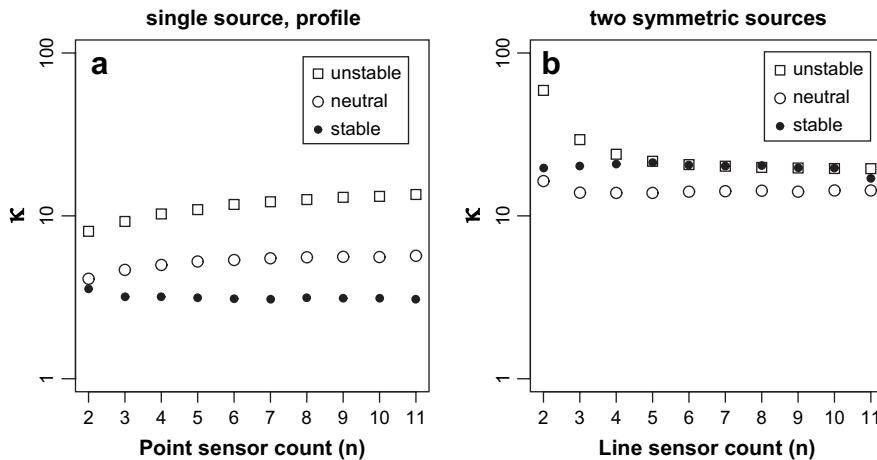
Fig. 10. Condition number vs. number of sensors for (a) the single-source profile geometry shown in Fig. 1c; (b) the symmetric double-source case with line sensors in Fig. 5b. In both cases, little if any benefit is provided by additional sensors distributed evenly between the outer sensors.

number. For example, the number of measurements can be increased to exceed the minimum required, in order to reduce the significance of particular measurements as the solution becomes ever less constrained by them. This can be accomplished either by adding more sensors or by incorporating data taken over a longer time period.

Although using more sensors and/or data may be helpful, it is prudent to minimize condition number as much as possible by careful sensor placement (as described above); as we have seen, adding an arbitrary number of poorly located sensors will be of little or no benefit. Data sets are finite and there are practical limits on the use of fitting procedures to obtain good solutions, particularly when source strengths are time-varying. A smoothness or similar constraint such as that introduced by Siqueira et al. (2000) is not possible in general, when no such relationship exists between independent sources.

It is sometimes advantageous that the atmospheric surface layer has a strong vertical asymmetry. Turbulent transport processes lead to marked changes with height in concentration at a given location (see Fig. 3). Measurements taken at different heights tend to be dissimilar and therefore improve the condition of the system. The same turbulent mixing causes concentration to become more uniform with height as the downwind distance from a source increases, decreasing the potential benefit of vertical inhomogeneity.

Our experiments have demonstrated that condition number for a given geometry can vary significantly with stratification. Mixing is suppressed under stable conditions, so that vertical concentration differences are maintained for longer fetches and concentration at a given level falls off less quickly with distance downwind of the source. Unstable conditions promote vertical mixing and more uniform profiles, while concentration decreases more rapidly with downwind fetch. Stability changes therefore make sensor placement more challenging, since an arrangement suitable for one stratification state might be less so for another.

Overall, we expect that having sensors widely spaced and possibly at different heights is a good practice where the background is unknown or multiple sources are present. It is an unfortunate reality that separating multiple sources is likely to be difficult if not impossible in some cases because sensors will have to be frequently repositioned to accommodate changes in wind direction and stratification.

The use of line-averaging concentration sensors complicates the task of isolating individual sources. Line sensors have excellent characteristics for measuring single sources: their concentrations provide a better average over the source plume and are therefore less susceptible to source variability; they reduce sensitivity to wind direction and increase the likelihood of the sensor intercepting the emitted plume; and they allow more frequent and accurate measurements because the (effective) gas concentration is amplified by the detector's path length. These same features can become liabilities where more than one source is present; their wider concentration footprint makes them more prone to intercepting multiple emissions, which will increase κ. It is likely to be more important to take advantage of vertical and horizontal asymmetries in concentration distribution when placing line-average instruments.

5. Conclusions

The influence on sensitivity to error from source–sensor geometry requires that we use great care in placing sensors when measuring multiple sources and might force us to relocate them as conditions change. The surface layer's variability greatly complicates the selection of a static sensor placement; a practical configuration under one wind direction, surface layer stability, and roughness length might be unworkable under different conditions. Adding more sensors is not guaranteed to improve the solutions, but their careful placement will do so.

Using numerical models to assess the response of condition number to a given placement of sensors under different atmospheric conditions might help determine a useful arrangement. Software could be adapted to automate the process of seeking optimum sensors' placement to minimize condition number for a given source configuration and range of wind directions and stabilities. Ideally, models would be run in real time to determine the expected condition number and sensors would be dynamically placed to accommodate changes as required.

References

Allen, C.T., Haupt, S.E., Young, G.S., 2007a. Source characterization with a genetic algorithm-coupled dispersion-backward model incorporating SCIPUFF. Journal of Applied Meteorology 46, 273–287.

Allen, C.T., Young, G.S., Haupt, S.E., 2007b. Improving pollutant source characterization by better estimating wind direction with a genetic algorithm. Atmospheric Environment 41, 2283–2289.

Flesch, T.K., Wilson, J.D., Yee, E., 1995. Backward-time Lagrangian stochastic dispersion models, and their application to estimate gaseous emissions. Journal of Applied Meteorology 34, 1320–1332.

Flesch, T.K., Wilson, J.D., Harper, L.A., Crenna, B.P., Sharpe, R.R., 2004. Deducing ground-air emissions from observed trace gas concentrations: a field trial. Journal of Applied Meteorology 43, 487–502.

Gentle, J.E., 1998. Numerical Linear Algebra for Applications in Statistics. Springer, New York.

Haupt, S.E., 2005. A demonstration of coupled receptor/dispersion modeling with a genetic algorithm. Atmospheric Environment 39, 7181–7189.

Haupt, S.E., Young, G.S., Allen, C.T., 2006. Validation of a receptor/dispersion model coupled with a genetic algorithm using synthetic data. Journal of Applied Meteorology 45, 476–490.

Hsieh, C.-I., Siqueira, M., Katul, G., Chu, C.-R., 2003. Predicting scalar source–sink and flux distributions within a forest canopy using a 2-D Lagrangian stochastic dispersion model. Boundary-Layer Meteorology 109, 113–138.

Leuning, R., Denmead, O.T., Miyata, A., Kim, J., 2000. Source/sink distributions of heat, water vapour, carbon dioxide and methane in a rice canopy estimated using Lagrangian dispersion analysis. Agricultural and Forest Meteorology 104, 233–249.

Noble, B., Daniel, J.W., 1988. Applied Linear Algebra. Prentice-Hall, New Jersey.

Press, W.H., Flannery, B.P., Teukolsky, S.A., Vetterling, W.T., 1986. Numerical Recipes: The Art of Scientific Computing. Cambridge University Press, New York.

Qiu, Guowang, Warland, J.S., 2006. Inferring profiles of energy fluxes within a soybean canopy using Lagrangian analysis. Agricultural and Forest Meteorology 139, 119–137.

Raupach, M.R., 1989a. A practical Lagrangian method for relating scalar concentrations to source distributions in vegetative canopies. Quarterly Journal of the Royal Meteorological Society 115, 609–632.

Raupach, M.R., 1989b. Applying Lagrangian fluid mechanics to infer scalar source distributions from concentration profiles in plant canopies. Agricultural and Forest Meteorology 47, 85–108.

Roussel, G., Delmaire, G., Ternisien, E., Lherbier, R., 2000. Separation problem of industrial particles emissions using a stationary scattering model. Environmental Modeling and Software 15, 653–661.

Scheick, J.T., 1996. Linear Algebra with Applications. McGraw-Hill, New York.

Siqueira, M., Lai, C.-T., Katul, G., 2000. Estimating scalar sources, sinks, and fluxes in a forest canopy using Lagrangian, Eulerian, and hybrid inverse models. Journal of Geophysical Research 105 (D24), 29,475–29,488.

Simon, E., Lehmann, B.E., Ammann, C., Ganzveld, L., Rummel, U., Meixner, F.X., Nobre, A.D., Araujo, A., Kesselmeier, J., 2005. Lagrangian dispersion of ^{222}Rn, H_2O, and CO_2 within Amazonian rain forest. Agricultural and Forest Meteorology 132, 286–304.

Wilson, J.D., Thurtell, G.W., Kidd, G.E., Beauchamp, E.G., 1982. Estimation of the rate of gaseous mass transfer from a surface source plot to the atmosphere. Atmospheric Environment 16, 1861–1867.

Wilson, J.D., Sawford, B.L., 1996. Lagrangian stochastic models for trajectories in the turbulent atmosphere. Boundary-Layer Meteorology 78, 191–210.

Wohlfahrt, G., 2004. Modeling fluxes and concentrations of CO_2, H_2O, and sensible heat within and above a mountain meadow canopy: a comparison of three Lagrangian models and three parameterization options for the Lagrangian time scale. Boundary-Layer Meteorology 113, 43–80.